UCLA
COMPUTATIONAL AND APPLIED MATHEMATICS

Multigrid, Alignment, and Euler's Equations

Wim A. Mulder

February 1989

CAM Report 89-05

Department of Mathematics
University of California, Los Angeles
Los Angeles, CA. 90024-1555

UCLA
COMPUTATIONAL AND APPLIED MATHEMATICS

Multigrid, Alignment, and Euler's Equations

Wim A. Mulder

February 1989

CAM Report 89-05

Department of Mathematics
University of California, Los Angeles
Los Angeles, CA. 90024-1555

Multigrid, alignment, and Euler's equations

Wim A. Mulder
Department of Mathematics
405 Hilgard Avenue
University of California at Los Angeles
Los Angeles, CA 90024-1555
Arpanet: mulder@math.ucla.edu

This work has been supported by NSF grants DMS85-03294 and DMS88-11863, and ONR grant N00014-86-K-0691.

February 28, 1989

To be presented at the Fourth Copper Mountain Conference on Multigrid Methods, April 9-13, 1989.

Multigrid, alignment, and Euler's equations*

Wim A. Mulder
Department of Mathematics
405 Hilgard Avenue
University of California at Los Angeles
Los Angeles, CA 90024-1555

The multigrid technique can be used to compute stationary solutions to Euler's equations of gas dynamics. To obtain some insight in the convergence behaviour, only the linearised equations with constant coefficients are considered in this paper. The spatial discretisation is obtained by first-, second-, or third-order upwind differencing. Convergence to the steady state can be hampered by alignment, the flow being aligned with the grid. A number of approaches to remove this problem are described. Acceptable convergence rates can be obtained for first-order schemes. Two-level analysis shows that higher-order schemes will hardly or not converge. This is caused by waves perpendicular to stream-lines. Because the exact operator vanishes for these waves, the poor convergence rates are due to the truncation error. It is shown that convergence to the level of the the truncation error can be easily obtained by defect correction, at least for the linear constant-coefficient case.

Key words: multigrid method, steady Euler equations, convergence

AMS (MOS) subject classifications: 35L65, 65N20, 76N15

1. Introduction

A problem in computing steady inviscid flow with the multigrid method is alignment, which occurs if a stream-line coincides with a grid-line [2,4]. This makes it difficult to remove oscillatory iteration errors (deviations from the steady state) perpendicular to the stream-line. Such waves can not be removed by smoothing, because there is no coupling in the perpendicular direction, nor can they be removed by a coarse-grid correction, because their oscillatory character does not allow their representation on coarser grids. The result is slow convergence.

One way to overcome alignment is the use of global relaxation schemes such as line relaxation or Gauss-Seidel. Note that the latter, although implemented as a local scheme, strongly affects the long waves, and is therefore classified as a global scheme. An alternative is the use of semi-coarsening, which allows for the construction of an $O(N)$ method that provides a nonlinear alternative for line relaxation [11]. This approach is reviewed in §2. An $O(N \log N)$ variant is presented as well. These two methods can not handle alignment at 45°, but that is not a problem for first-order upwind schemes.

Linear two-level analysis can be used to gain insight in the convergence behaviour of the multigrid method. Here we will compute two-level convergence rate for the linear constant-coefficient case. Although this is a major simplification with respect to the nonlinear case, the study can identify bottlenecks for fast convergence.

The upwind differencing of the linearised Euler equations with constant coefficients is described in §3, and is used for the two-level convergence analysis in §4. It turns out that second-order schemes will not convergence at all, and third-order schemes only barely. However, convergence to the level of the truncation error can be easily obtained by defect correction, as demonstrated in §5.

* *This work has been supported by NSF grants DMS85-03294 and DMS88-11863, and ONR grant N00014-86-K-0691.*

2. Alignment

The multigrid method allows the computation of solutions to certain partial differential equations in $O(N)$ operations. Its three basic ingredients are: smoothing, coarse-grid correction, and successive grid-refinement. Smoothing removes high-frequency components of the iteration error, that can not be represented on coarser grids. Because these high frequencies are related to the local structure of the solution, they can often easily be removed. The low frequencies are accounted for by corrections to the solution computed on coarser grids. The lower frequencies appear as high frequencies on sufficiently coarse grids, and can be removed easily as well. This leads to a convergence rate independent of grid size. Successive grid-refinement is required to obtain a good initial guess on each currently finest grid. Otherwise, $O(\log N)$ iterations would be required to reduce an initial $O(1)$ iteration error to the size of the discretisation error. With successive grid-refinement, the complexity becomes $O(N)$ [2,4].

Alignment is one cause of failure for the multigrid method. This occurs if the equations become decoupled in one of the coordinate directions. In that case, a high-frequency iteration error can not be removed by smoothing, because there is no coupling, nor by the coarse-grid correction, because high frequencies can not be represented on coarser grids. This phenomenon is well known, and occurs for instance for strongly anisotropic elliptic equations [2,4]. For flow problems, it is the rule rather than the exception, because stream-lines are one-dimensional in nature.

An obvious remedy against alignment is the use of global relaxation schemes. The term "global" refers to the effect of the relaxation scheme: here it is called "global" if the long waves are affected, and "local" otherwise. Thus, line relaxation and Gauss-Seidel relaxation are both global schemes, despite the fact that the latter is implemented as a local operation. For the first-order upwind-differenced Euler equations, Gauss-Seidel relaxation is not good enough as global solver, as is demonstrated in [8] by linear two-level analysis and nonlinear experiments. The problem of alignment disappears only for the hyperbolic component of the equations. Damped Alternating Direction Line Jacobi relaxation is able to provide uniformly good convergence rates, according to the linear two-level analysis in [10]. A convergence rate of 0.526 was found. It still remains to be seen if a comparable figure can be obtained in the nonlinear case.

A nonlinear alternative to line relaxation is described in [11]. This method uses semi-coarsening in two or three coordinate directions simultaneously. An example of the data-structure for the two-dimensional case is shown in Fig. 1, where the finest grid is 8×8 and the coarsest 1×1. The number of cells involved is $2^d N$, if the number of cells on the finest grid is N in a d-dimensional problem. The cost of a V-cycle is proportional to this number, that of an F-cycle is a factor $(d+1)$ larger. For W-cycles, the $O(N)$ complexity is lost. It is clear from Fig. 1 that the usual restriction and prolongation operators must be modified if data from more than one grid are combined. A simple method is proposed in [11]. Equal weighting is used for the restriction of data from more than one grid. For prolongation, the correction to the solution on the current fine grid is computed with respect to the latest solution available rather than the one at the begin of the multigrid cycle. This allows for smoothing parallel to the computation of the coarse-grid correction, if desired.

The extension of this method to three dimensions is obvious, as is its formulation in a finite-difference instead of a finite-volume context. The approach is not tied to a specific type of equation, although in [11] it is only studied for the two-dimensional Euler equations. In that case, linear two-level analysis for the constant-coefficient case provides a two-grid convergence factor that is at worst 0.5 if first-order upwind differencing is used. Experiments on the nonlinear equations show multi-level convergence rates that are somewhat better. It should be noted that this method can not handle alignment at 45°, which is obviously not a problem here.

A variant of the method that requires only $2N$ cells rather than $2^d N$, can be obtained by semi-coarsening in a sequential fashion. First a coarse-grid correction based on coarsening in one coordinate direction is computed and the fine-grid solution is updated. Then the same is done

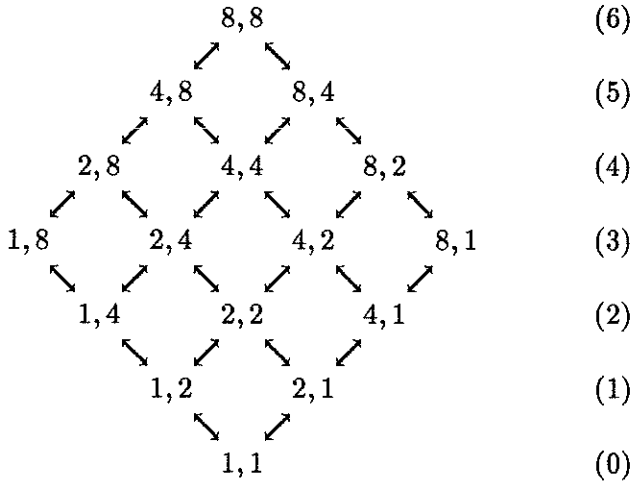

Fig. 1. *Arrangement of finest (8×8) and coarser grids, that leads to an $O(N)$ multigrid method for problems with alignment. The level numbers are given on the right. The arrows indicate how the grids are linked by restriction (downward) and prolongation (upward).*

in the other coordinate direction. Here it is assumed that the problem is two-dimensional. With this approach, the restriction and prolongation operator do not have to be modified to handle data from more than one grid at the time. A disadvantage is its complexity. Two coarse-grid corrections have to be computed with respect to each grid during the multigrid cycle, which leads to at least $O(N \log N)$ operations per cycle. Two-level analysis for the linear constant-coefficient case provides a worst-case two-level convergence rate of 0.5, although the overall performance is somewhat better than with the previous method.

Both the original $O(N)$ method and the $O(N \log N)$ variant have the potential to be considerably accelerated by pruning the data-structure. This requires adaptivity based on flow direction and convergence speed, and remains to be investigated. In the following, we will only consider the $O(N)$ method, and not its $O(N \log N)$ variant.

In summary, steady solutions to Euler's equations can be computed in a straightforward manner if first-order upwind differencing is used, at least according the two-level analysis in the linear constant-coefficient case. The numerical experiments reported in [11] suggest that this conclusion extends to the nonlinear case. In the remainder of this paper, we will focus on second- and third-order upwind discretisations of Euler's equations.

3. Upwind differencing

The Euler equations of gas dynamics that describe the flow of a perfect inviscid compressible gas are:

$$\frac{\partial w}{\partial t} + \frac{\partial f}{\partial x} + \frac{\partial g}{\partial y} = 0. \tag{3.1a}$$

Here the vector of states w and the fluxes f and g are given by

$$w = \begin{pmatrix} \rho \\ \rho u \\ \rho v \\ \rho E \end{pmatrix}, \quad f = \begin{pmatrix} \rho u \\ \rho u^2 + p \\ \rho uv \\ \rho uH \end{pmatrix}, \quad g = \begin{pmatrix} \rho v \\ \rho uv \\ \rho v^2 + p \\ \rho vH \end{pmatrix}. \tag{3.1b}$$

The density is denoted by ρ, and u and v are the x- and y-component of the velocity. The energy E, total enthalpy H, pressure p, and sound speed c are related by

$$E = \frac{1}{\gamma - 1}\frac{p}{\rho} + \tfrac{1}{2}(u^2 + v^2), \quad H = E + \frac{p}{\rho}, \quad c^2 = \gamma\frac{p}{\rho}. \tag{3.1c}$$

The spatial part of the system is discretised by upwind differencing. The discrete residual is

$$\begin{aligned} r_{i,j} = &- \frac{1}{h_x}\left[f(w(q_{i,j}^{i+}), w(q_{i+1,j}^{i-})) - f(w(q_{i-1,j}^{i+}), w(q_{i,j}^{i-}))\right] \\ &- \frac{1}{h_y}\left[g(w(q_{i,j}^{j+}), w(q_{i,j+1}^{j-})) - g(w(q_{i,j-1}^{j+}), w(q_{i,j}^{j-}))\right]. \end{aligned} \tag{3.2a}$$

Here $f(w_l, w_r)$ and $g(w_l, w_r)$ are numerical fluxes that provide an exact or approximate solution to the Riemann problem. The expression $w(q)$ denotes a one-to-one transformation from a set of state quantities q to w. The quantities $q_{i,j}^{i\pm}$ and $q_{i,j}^{j\pm}$ are values at the cell-boundaries obtained by interpolation from the state $q_{i,j} = q(w_{i,j})$. A first-order-accurate scheme is obtained if the interpolated values simply equal the interior values. Second-order accuracy is obtained by using van Leer's kappa-scheme [1,14], which lets, in the x-direction,

$$\begin{aligned} q_{i,j}^{i+} &= q_{i,j} + \tfrac{1}{4}s(\Delta_{i,j}^{i-}, \Delta_{i,j}^{i+})\left[(1-\kappa)\Delta_{i,j}^{i-} + (1+\kappa)\Delta_{i,j}^{i+}\right], \\ q_{i,j}^{i-} &= q_{i,j} - \tfrac{1}{4}s(\Delta_{i,j}^{i-}, \Delta_{i,j}^{i+})\left[(1-\kappa)\Delta_{i,j}^{i+} + (1+\kappa)\Delta_{i,j}^{i-}\right]. \end{aligned} \tag{3.3a}$$

Here

$$\Delta_{i,j}^{i-} = q_{i,j} - q_{i-1,j}, \quad \Delta_{i,j}^{i+} = q_{i+1,j} - q_{i,j}. \tag{3.3b}$$

The function $s(\Delta^-, \Delta^+)$ is a limiter that prevents numerical oscillations, and takes values between 0 and 1. Expression similar to (3.3) are used for the y-direction.

The standard second-order upwind scheme (Fromm's scheme) is obtained for $\kappa = 0$. Central differencing is obtained for $\kappa = 1$, if the limiter is not used ($s(\Delta^-, \Delta^+) = 1$). The choice $\kappa = -1$ provides a fully one-sided upwind scheme. The limiter may cause the accuracy to reduce to first-order at isolated points. For $\kappa = 1/3$, we obtain third-order accuracy in a point-wise sense, but not in a volume-averaged sense. The reason is that there is a second-order difference between point-values and volume-averages. Also, the flux of the average state is not equal to the average of the flux over one part of the cell boundary. A local $O(1)$ error occurs if a steady discontinuity is smeared out over a number of cells. Thus, we have at most second-order accuracy in large regions of the flow, and first-order or even zero-order accuracy at isolated points or lines. For this reason, the discretisation is referred to as a *high-resolution* scheme. An additional problem occurs if the grid is not locally Cartesian or if cell-sizes vary strongly from one cell to another. Then the one-dimensional interpolation (3.3) should be corrected for stretching and curvature. Here we have assumed that the grid is Cartesian without stretching from cell to cell. Note that the aspect ratio h_y/h_x of the cells is not involved in this discussion: it may be far away from 1.

In the next section, we will attempt to construct a multigrid method for the high-resolution scheme described above. In order to obtain estimates for the convergence rate, we make the following simplifying assumptions. The nonlinear scheme is replaced by a linear with constant coefficients. We assume that the grid is Cartesian with a fixed cell-size h_x in the x-direction and h_y in the y-direction. The effect of the limiter is ignored. Boundary conditions are assumed to be periodic. We only consider the finest grid and one or two grids on the next coarser level. It is assumed that the coarse-grid problem is solved exactly. In this setting, we can use Fourier analysis. Although the assumptions have brought us quite far from the original problem, the idealized case

can nevertheless reveal the strength and weaknesses of the multigrid method, and provide some numbers which can serve as a reference for the nonlinear case.

The following linearised version of (3.1) is adopted:

$$\frac{\partial w'}{\partial t} + A\frac{\partial w'}{\partial x} + B\frac{\partial w'}{\partial y} = 0, \tag{3.4a}$$

where

$$A = \begin{pmatrix} u & 0 & c & 0 \\ 0 & u & 0 & 0 \\ c & 0 & u & 0 \\ 0 & 0 & 0 & u \end{pmatrix}, \quad B = \begin{pmatrix} v & 0 & 0 & 0 \\ 0 & v & c & 0 \\ 0 & c & v & 0 \\ 0 & 0 & 0 & v \end{pmatrix}, \quad \delta w' = \begin{pmatrix} \delta u \\ \delta v \\ \delta p/(\rho c) \\ \delta S \end{pmatrix}. \tag{3.4b}$$

Here $S = \log(p/\rho^\gamma)$ is the specific entropy. The fourth equation describes the convection of entropy along stream-lines. The remaining 3×3 system represents the combination of convection and sound waves. In the isentropic case, the fourth equation can be dropped and the third component of w' becomes $2c/\gamma_1$. For the steady-state problem, we consider the linear residual operator

$$L = A\frac{\partial}{\partial x} + B\frac{\partial}{\partial y}, \tag{3.5}$$

with constant coefficients and periodic boundary conditions. This operator is elliptic in the subsonic and hyperbolic in the supersonic case. The fourth equation, considered by itself, is hyperbolic.

To accomplish the upwind differencing, the matrix A is diagonalised by Q_1, according to

$$A = Q_1 \Lambda_1 Q_1^{-1}, \quad \Lambda_1 = \mathrm{diag}(u-c, u, u, u+c), \quad Q_1 = \begin{pmatrix} 1 & 0 & 0 & 1 \\ 0 & -1 & 0 & 0 \\ -1 & 0 & 0 & 1 \\ 0 & 0 & 1 & 0 \end{pmatrix}. \tag{3.6a}$$

For B we have:

$$B = Q_2 \Lambda_2 Q_2^{-1}, \quad \Lambda_2 = \mathrm{diag}(v-c, v, v, v+c), \quad Q_2 = \begin{pmatrix} 0 & 1 & 0 & 0 \\ 1 & 0 & 0 & 1 \\ -1 & 0 & 0 & 1 \\ 0 & 0 & 1 & 0 \end{pmatrix}. \tag{3.6b}$$

The matrix Λ_k $(k = 1, 2)$ is split into Λ_k^+ and Λ_k^-, which contain the positive and negative elements of Λ_k, respectively. This implies

$$\Lambda_k^+ + \Lambda_k^- = \Lambda_k, \quad \Lambda_k^+ - \Lambda_k^- = |\Lambda_k|. \tag{3.7}$$

Now define

$$A^\pm \equiv Q_1 \Lambda_1^\pm Q_1^{-1}, \quad B^\pm \equiv Q_2 \Lambda_2^\pm Q_2^{-1}. \tag{3.8}$$

It follows that

$$\begin{aligned} A = A^+ + A^-, \quad |A| \equiv Q_1 |\Lambda_1| Q_1^{-1} = A^+ - A^-; \\ B = B^+ + B^-, \quad |B| \equiv Q_2 |\Lambda_2| Q_2^{-1} = B^+ - B^-. \end{aligned} \tag{3.9}$$

The discrete linear residual operator becomes

$$L^{h_x,h_y}(T_x, T_y) = L_x^{h_x}(T_x) + L_y^{h_y}(T_y), \tag{3.10a}$$

where

$$L_x^{h_x}(T_x) = \frac{1}{h_x}[A^+ D(T_x, s_x, \kappa) - A^- D(T_x^{-1}, s_x, \kappa)],$$
$$L_y^{h_y}(T_y) = \frac{1}{h_y}[B^+ D(T_y, s_y, \kappa) - B^- D(T_y^{-1}, s_y, \kappa)], \tag{3.10b}$$

and

$$D(T, s, \kappa) = (1 - T^{-1}) \left[1 + \tfrac{1}{4} s \left((1-\kappa)(1-T^{-1}) + (1+\kappa)(T-1)\right)\right]. \tag{3.10c}$$

Here T_x and T_y are shift operators: $T_x v_{i,j} = v_{i+1,j}$, $T_y v_{i,j} = v_{i,j+1}$. We have assumed that the grid is Cartesian with a constant aspect ratio h_y/h_x. First-order accuracy is obtained for $s_x = s_y = 0$. For $s_x = s_y = 1$ and $|\kappa| \leq 1$, we have a high resolution scheme. The scheme is third-order for $\kappa = 1/3$ in a point-wise sense. Other values of κ lead to second-order accuracy.

The analysis will be carried in Fourier space. We consider Fourier modes of the form

$$\exp\left[-\mathrm{i}\,(i\theta_x + j\theta_y)\right], \tag{3.11a}$$

where the frequencies on a $N_1 \times N_2$ grid are

$$\theta_x = 2\pi \frac{l_1}{N_1}, \quad \theta_y = 2\pi \frac{l_2}{N_2}, \quad l_1 = 0, \ldots, N_1 - 1, \quad l_2 = 0, \ldots, N_2 - 1. \tag{3.11b}$$

The symbols of the shift operators are $\hat{T}_x = \exp(\mathrm{i}\theta_x)$ and $\hat{T}_y = \exp(\mathrm{i}\theta_y)$. The symbol of the residual operator is obtained from (3.10) by replacing T_x and T_y with $\hat{T}_x$ and $\hat{T}_y$. In that case, we have

$$\begin{aligned} \mathrm{Re}\,\hat{D}(\hat{T}, s, \kappa) &= 2\zeta\left[1 - s + s(1-\kappa)\zeta\right], \quad \zeta = \sin^2(\tfrac{1}{2}\theta), \\ \mathrm{Im}\,\hat{D}(\hat{T}, s, \kappa) &= \sin(\theta)\left[1 + s(1-\kappa)\zeta\right]. \end{aligned} \tag{3.12}$$

The singularities of the linear operator $\hat{L}^{h_x, h_y}$ are listed in the Appendix.

4. Linear two-level analysis

4.1. Two-grid operators

The convergence of the $O(N)$ multigrid method described in Sect. 2 can be studied by two-level analysis [2,4]. As mentioned before, we consider the linear constant-coefficient case with periodic boundary conditions. Only two levels are considered, a fine and a coarse; it is assumed that the equations on the coarse grid are solved exactly. This leads to the coarse-grid correction operator, which describes how the exact solution on the coarser level affects the convergence on the finest grid. Note that we make a distinction between "grid" and "level", as the method described in Sect. 2 may involve more than one grid on a given level. Here we have one finest grid and 2 coarser grids on the next level. The finest grid has a size $N_1 \times N_2$, N_1 and N_2 even. Semi-coarsening in the x-direction leads to a $(N_1/2) \times N_2$ grid. The corresponding coarse-grid correction operator will be denoted by K^{Hh}. An $N_1 \times (N_2/2)$ grid is obtained by semi-coarsening in the y-direction, and the corresponding operator is K^{hH}. We will also consider the usual coarse-grid correction operator K^{HH} that is obtained by coarsening in both the x- and y-direction.

In the Fourier domain, coarsening causes aliasing between frequencies: θ_x is coupled to $\theta_x + \pi$ by coarsening in x, and θ_y is coupled to $\theta_y + \pi$ by coarsening in y. Therefore, we consider 4 frequencies at once, using the following notation:

$$\hat{\mathbf{v}} = \begin{pmatrix} \hat{v}_{++} \\ \hat{v}_{-+} \\ \hat{v}_{+-} \\ \hat{v}_{--} \end{pmatrix} \equiv \begin{pmatrix} \hat{v}(\theta_x & , \theta_y &) \\ \hat{v}(\theta_x + \pi & , \theta_y &) \\ \hat{v}(\theta_x & , \theta_y + \pi &) \\ \hat{v}(\theta_x + \pi & , \theta_y + \pi &) \end{pmatrix}, \quad |\theta_x| \leq \tfrac{1}{2}\pi, \quad |\theta_y| \leq \tfrac{1}{2}\pi. \tag{4.1}$$

which consists of the symbols of a vector v for 4 waves. The corresponding symbol for a linear operator G will have the structure

$$\hat{\mathbf{G}} = \begin{pmatrix} \hat{G}_{1++} & \hat{G}_{2++} & \hat{G}_{3++} & \hat{G}_{4++} \\ \hat{G}_{2-+} & \hat{G}_{1-+} & \hat{G}_{4-+} & \hat{G}_{3-+} \\ \hat{G}_{3+-} & \hat{G}_{4+-} & \hat{G}_{1+-} & \hat{G}_{2+-} \\ \hat{G}_{4--} & \hat{G}_{3--} & \hat{G}_{2--} & \hat{G}_{1--} \end{pmatrix}, \tag{4.2}$$

where each entry corresponds to a 4×4 block. The residual operator on the fine grid becomes:

$$\hat{\mathbf{L}}^{hh} = \mathrm{diag}(\hat{L}^{h_x,h_y}_{++}, L^{h_x,h_y}_{-+}, \hat{L}^{h_x,h_y}_{+-}, \hat{L}^{h_x,h_y}_{--}). \tag{4.3}$$

For the restriction operators, we consider either first-order or third-order coarsening:

$$R_1(T) = \tfrac{1}{2}(1+T), \tag{4.4a}$$
$$R_3(T) = \tfrac{1}{8}T^{-1}(1+T)^3. \tag{4.4b}$$

The three restriction operators, corresponding to the three different types of coarsening mentioned above, are:

$$\hat{\mathbf{R}}^{Hh} = \begin{pmatrix} R(\hat{T}_x) & R(-\hat{T}_x) & 0 & 0 \\ 0 & 0 & 0 & 0 \\ 0 & 0 & R(\hat{T}_x) & R(-\hat{T}_x) \\ 0 & 0 & 0 & 0 \end{pmatrix}, \quad \hat{\mathbf{R}}^{hH} = \begin{pmatrix} R(\hat{T}_y) & 0 & R(-\hat{T}_y) & 0 \\ 0 & R(\hat{T}_y) & 0 & R(-\hat{T}_y) \\ 0 & 0 & 0 & 0 \\ 0 & 0 & 0 & 0 \end{pmatrix}, \tag{4.5a}$$

and

$$\hat{\mathbf{R}}^{HH} = \hat{\mathbf{R}}^{Hh}\hat{\mathbf{R}}^{hH} = \hat{\mathbf{R}}^{hH}\hat{\mathbf{R}}^{Hh}. \tag{4.5b}$$

For $R(T)$, either of the opertors in (4.4) will be considered. The prolongation operators $\hat{\mathbf{P}}^{Hh}$, $\hat{\mathbf{P}}^{hH}$, and $\hat{\mathbf{P}}^{HH}$, equal the conjugate transposes of the corresponding restriction operators.

To obtain the two-level coarse-grid correction operators for each of the three types of coarsening, we need the residuals on the coarser grids:

$$\begin{aligned} \hat{\mathbf{L}}^{Hh} &= \mathrm{diag}(\hat{L}^{2h_x,h_y}(\hat{T}_x^2, \hat{T}_y), 0, \hat{L}^{2h_x,h_y}(\hat{T}_x^2, -\hat{T}_y), 0), \\ \hat{\mathbf{L}}^{hH} &= \mathrm{diag}(\hat{L}^{h_x,2h_y}(\hat{T}_x, \hat{T}_y^2), \hat{L}^{h_x,2h_y}(-\hat{T}_x, \hat{T}_y^2), 0, 0), \\ \hat{\mathbf{L}}^{HH} &= \mathrm{diag}(\hat{L}^{2h_x,2h_y}(\hat{T}_x^2, \hat{T}_y^2), 0, 0, 0). \end{aligned} \tag{4.6}$$

The coarse-grid correction operators K^{Hh}, K^{hH}, and K^{HH}, are defined by

$$K = I - P(L^H)^\dagger R L^{hh}, \tag{4.7}$$

the appropriate substitutions being obvious for each of the three cases. The dagger denotes the pseudo-inverse. The two-grid matrices, corresponding to the $O(N)$ method described in §2 and [11], are

$$\begin{aligned} M^{(1)} &= S^{\nu_2}[K^{(1)} + (I - \tilde{P}^{Hh}\tilde{R}^{Hh})(I - \tilde{P}^{hH}\tilde{R}^{hH})(S^{\nu_p} - I)]S^{\nu_1}, \\ M^{(2)} &= S^{\nu_2}[K^{(2)} + (I - \tilde{P}^{hH}\tilde{R}^{hH})(I - \tilde{P}^{Hh}\tilde{R}^{Hh})(S^{\nu_p} - I)]S^{\nu_1}, \end{aligned} \tag{4.8a}$$

where

$$\begin{aligned} K^{(1)} &= K^{Hh} + (I - \tilde{P}^{Hh}\tilde{R}^{Hh})(K^{hH} - I), \\ K^{(2)} &= K^{hH} + (I - \tilde{P}^{hH}\tilde{R}^{hH})(K^{Hh} - I). \end{aligned} \tag{4.8b}$$

The smoothing operator S is applied ν_1 times for pre-smoothing, ν_p times for parallel smoothing, and ν_2 times for post-smoothing. The operators $\tilde{R}$ and $\tilde{P}$ may or may not be the same as the R and P used for the coarse-grid correction operator. Because the smoothing operator will in general be inefficient for the long waves ($S \simeq I$), the multigrid convergence for these waves is mainly determined by $K^{(1)}$ and $K^{(2)}$.

4.2. Stability of the coarse-grid correction operators

To obtain a good multigrid convergence, we require the coarse-grid correction operators to be stable and have a good low-frequency damping. Stability requires $\|\hat{\mathbf{K}}\| \leq 1$, although a bounded norm larger than one may be allowed if smoothing can compensate the growth of the corresponding waves. Here we use the seminorm

$$\|\hat{\mathbf{G}}\| \equiv \max\left\{\rho\left(\hat{\mathbf{L}}^{h_x,h_y}\hat{\mathbf{G}}\,(\hat{\mathbf{L}}^{h_x,h_y})^{\dagger}\right) : u/c, v/c, h_y/h_x, \theta_x, \theta_y\right\}, \tag{4.9}$$

where $\rho(\cdot)$ denotes the spectral radius. A similarity transform based on $\hat{\mathbf{L}}^{h_x,h_y}$ is included to mask out the effect of singularities. The dagger indicates the pseudo-inverse. The matrices considered here depend on 5 parameters: the velocities u/c and v/c, the grid aspect ratio h_y/h_x, and the frequencies θ_x, θ_y. For the norm we will use the maximum over these five parameters, unless specified otherwise.

To determine the stability of $\hat{\mathbf{K}}^{HH}$, a similarity transform based on the non-singular matrix

$$\hat{\mathbf{Q}}^{HH} = \begin{pmatrix} \hat{\mathbf{P}}^{HH}_{1,1} & 0 & 0 & 0 \\ \hat{\mathbf{P}}^{HH}_{2,1} & I & 0 & 0 \\ \hat{\mathbf{P}}^{HH}_{3,1} & 0 & I & 0 \\ \hat{\mathbf{P}}^{HH}_{4,1} & 0 & 0 & I \end{pmatrix} \tag{4.10}$$

is carried out, yielding

$$(\hat{\mathbf{Q}}^{HH})^{-1}(\mathbf{I} - \hat{\mathbf{K}}^{HH})\hat{\mathbf{Q}}^{HH} = \begin{pmatrix} (\hat{\mathbf{L}}^{HH}_{1,1})^{\dagger}(\hat{\mathbf{R}}^{HH}\hat{\mathbf{L}}^{hh}\hat{\mathbf{P}}^{HH})_{1,1} & * & * & * \\ 0 & 0 & 0 & 0 \\ 0 & 0 & 0 & 0 \\ 0 & 0 & 0 & 0 \end{pmatrix}. \tag{4.11}$$

The stars denote elements which are irrelevant in the present discussion. We immediately find that

$$\|\hat{\mathbf{K}}^{HH}\| = \max(\,1,\, \|I - (\hat{\mathbf{L}}^{HH}_{1,1})^{\dagger}(\hat{\mathbf{R}}^{HH}\hat{\mathbf{L}}^{hh}\hat{\mathbf{P}}^{HH})_{1,1}\|). \tag{4.12}$$

If the residual on the coarser grid is identical to the one obtained by Galerkin coarsening, we have $\hat{\mathbf{L}}^{HH} = \hat{\mathbf{R}}^{HH}\hat{\mathbf{L}}^{hh}\hat{\mathbf{P}}^{HH}$, and the coarse-grid correction operator is stable. For the first-order restriction and prolongation operators, this happens for the first-order residual, and for the second-order residual if $\kappa = 1$. The same result is found for $\hat{\mathbf{K}}^{Hh}$ and $\hat{\mathbf{K}}^{hH}$.

For the higher-order residual with $\kappa \neq 1$, and the first-order restriction and prolongation operators, we find that $\hat{\mathbf{K}}$ is *unstable*. To demonstrate this, we only consider the fourth equation of (3.4), so that $\hat{\mathbf{K}}$ becomes a 4×4 matrix with scalar entries. For $s_x = s_y = 1$, $v/h_y = u/h_x$, $\kappa \neq 1$, and $\theta_y = -\theta_x$, we obtain

$$\|\hat{\mathbf{K}}^{HH}\| = \max_{\theta_x}(1, |(1 + \hat{T}_x^4)/(1 - \hat{T}_x^2)^2|), \tag{4.13a}$$

and

$$\|\hat{\mathbf{K}}^{Hh}\| = \|\hat{\mathbf{K}}^{hH}\| = \max_{\theta_x}(1, \left|\frac{3(1-\kappa)(1+\hat{T}_x)^2}{(1-\hat{T}_x)[2(1-\hat{T}_x)(1+2\hat{T}_x)^2 + (1-3\kappa)(1+3\hat{T}_x+3\hat{T}_x^2-\hat{T}_x^3)]}\right|). \tag{4.13b}$$

These norms blow up if θ_x approaches zero, i.e., for the long waves. The same happens to $\|\hat{\mathbf{K}}^{(1)}\| = \|\hat{\mathbf{K}}^{(2)}\|$.

At first sight, this is a surprising result. The general rule for the orders m_r of the restriction and m_p of the prolongation operator is [2,4]:

$$m_r + m_p \geq m, \tag{4.14}$$

where m is the order of the differential equation. This is supposed to guarantee stability, or at least boundedness of the coarse-grid correction operator. In this case $m = 1$, so the rule is obeyed, but the coarse-grid correction operator is unstable. However, closer inspection reveals that the rule is *not* violated. What happens is that the above choice of parameters describes a situation where the exact residual operator vanishes, so one basically looks at the truncation error. Since the truncation error can be viewed as a discretisation of a higher-order differential equation, we effectively have a value $m > 1$ for certain waves.

This can be illustrated by considering the Taylor expansion around $\theta_x = 0$, $\theta_y = 0$. For the fourth equation on the finest grid, with $u > 0$, $v > 0$, and $s_x = s_y = 1$, we have

$$\hat{L}^{h_x,h_y} \simeq \mathrm{i}(\tilde{u}\theta_x + \tilde{v}\theta_y) + \tfrac{1}{4}\mathrm{i}(\tfrac{1}{3} - \kappa)(\tilde{u}\theta_x^3 + \tilde{v}\theta_y^3) + \tfrac{1}{8}(1-\kappa)(\tilde{u}\theta_x^4 + \tilde{v}\theta_y^4), \tag{4.15a}$$

where

$$\tilde{u} = u/h_x, \quad \tilde{v} = v/h_y. \tag{4.15b}$$

The first-order term represents the exact operator. The second-order term vanishes and we have second-order accuracy. If, in addition, $\kappa = 1/3$, the third-order term vanishes as well, and third-order accuracy is obtained. For the special choice $\tilde{u}\theta_x = -\tilde{v}\theta_y$, the exact operator vanishes. What remains is due to the truncation error:

$$\hat{L}^{h_x,h_y} \simeq \tfrac{1}{4}\mathrm{i}(\tfrac{1}{3} - \kappa)\tilde{u}\theta_x(\theta_x^2 - \theta_y^2) + \tfrac{1}{8}(1-\kappa)\tilde{u}\theta_x(\theta_x^3 - \theta_y^3). \tag{4.16a}$$

For $\theta_y = -\theta_x$, we get

$$\tfrac{1}{4}(1-\kappa)\tilde{u}\theta_x^4, \tag{4.16b}$$

which can be considered as the discretisation of a *fourth-order* differential equation. Thus, the rule (4.14) is violated for this special wave.

A stable coarse-grid correction operator can be obtained with the third-order restriction (4.4b). If this one in used in combination with the first-order prolongation operator, the rule (4.14) is obeyed, and we expect boundedness of the coarse-grid correction operators. Indeed, numerical computations suggest that $\|\hat{\mathbf{K}}^{HH}\| \leq 1$ for $\kappa = 1$, $1/3$, 0, and -1. However, $\|\hat{\mathbf{K}}^{Hh}\| = \|\hat{\mathbf{K}}^{hH}\|$ and $\|\hat{\mathbf{K}}^{(1)}\| = \|\hat{\mathbf{K}}^{(2)}\|$ still are unbounded, except for $\kappa = 1/3$. To illustrate the problem, we consider

$$\|\mathbf{K}^{Hh}\| = \max(1, |I - (\hat{L}^{Hh})^{\dagger}(\hat{\mathbf{R}}^{Hh}\hat{\mathbf{L}}^{hh}\hat{\mathbf{P}}^{Hh})_{1,1}|). \tag{4.17}$$

For the long waves, we can examine the Taylor expansion around $\theta_x = 0$, $\theta_y = 0$. Both for $\hat{L}^{Hh}$ and $(\hat{\mathbf{R}}^{Hh}\hat{\mathbf{L}}^{hh}\hat{\mathbf{P}}^{Hh})_{1,1}$, the dominant term will be the exact operator, unless the latter becomes small. If we consider the fourth equation with $\tilde{u} > 0$, $\tilde{v} > 0$, and the choice of parameters $\tilde{u}\theta_x = -\tilde{v}\theta_y$, then the exact operator vanishes and what remains is

$$\begin{aligned} \hat{L}^{Hh} &\simeq \tfrac{1}{4}\mathrm{i}(\kappa - \tfrac{1}{3})\tilde{u}\theta_x(\theta_y^2 - 4\theta_x^2), \\ (\hat{\mathbf{R}}^{Hh}\hat{\mathbf{L}}^{hh}\hat{\mathbf{P}}^{Hh})_{1,1} &\simeq \tfrac{1}{4}\mathrm{i}(\kappa - \tfrac{1}{3})\tilde{u}\theta_x(\theta_y^2 - \ \theta_x^2), \end{aligned} \tag{4.18}$$

The residual on the coarser grid vanishes for $\theta_y = \pm 2\theta_x$, whereas the residual obtained by Galerkin coarsening vanishes in the same way as the fine-grid residual, namely for $\theta_y = \pm\theta_x$. This mismatch

cause the instability: if $\theta_y \simeq \pm 2\theta_x$, the norm (4.17) blows up. The instability can not be removed by using higher-order restriction and prolongation operators (with an order larger than 3), but disappears if $\kappa = 1/3$.

The instability for the second-order scheme can be removed by returning to the first-order restriction operator for the residual, and using a coarse-grid residual operator which is first-order in the direction in which one has coarsened. Thus,

$$\begin{aligned} \hat{L}^{Hh} &= \hat{L}^{2h_x}(\hat{T}_x^2, s_x = 0) + \hat{L}^{h_y}(\hat{T}_y, s_y = 1), \\ \hat{L}^{hH} &= \hat{L}^{h_x}(\hat{T}_x, s_x = 1) + \hat{L}^{2h_y}(\hat{T}_y^2, s_y = 0), \end{aligned} \tag{4.19}$$

and $\hat{L}^{HH}$ is the first-order operator. For these choices, and for the fourth equation of the system with $\tilde{u} > 0$, $\tilde{v} > 0$, we obtain

$$\begin{aligned} \hat{L}^{Hh} &\simeq \mathrm{i}(\tilde{u}\theta_x + \tilde{v}\theta_y) + \tilde{u}\theta_x^2, \\ (\hat{\mathbf{R}}^{Hh}\hat{\mathbf{L}}^{hh}\hat{\mathbf{P}}^{Hh})_{1,1} &\simeq \mathrm{i}(\tilde{u}\theta_x + \tilde{v}\theta_y) + \tfrac{1}{2}(1-\kappa)\tilde{u}\theta_x^2, \end{aligned} \tag{4.20}$$

and no problems occur if the exact operator vanishes, given $|\kappa| \leq 1$.

In summary, we can obtain stable coarse-grid correction operators for the second-order scheme if we use the first-order restriction and prolongation operators, and coarse-grid residuals that are first-order in the direction one has coarsened. For the third-order scheme, stability can also be obtained by using a third-order coarse-grid residual operator, and a third-order restriction operator for the residual. The other restriction ($\tilde{R}$) and prolongation operators ($P, \tilde{P}$) can still be first-order.

4.3. Low-frequency damping

Apart from stability, we also want a good damping of the low frequencies. This can be measured by those elements on the main diagonal of $\hat{\mathbf{K}}$ that correspond to the longest waves. In case of $\hat{\mathbf{K}}^{H,H}$, we have to consider $\hat{\mathbf{K}}_{1,1}^{H,H}$ for θ_x and θ_y close to zero. The subscripts refer to the left upper block of the matrix. We define

$$\psi(\hat{\mathbf{K}}) = \lim_{\varepsilon \to 0} \sup \left\{ \|\hat{\mathbf{K}}_{1,1}\| : \theta_x^2 + \theta_y^2 < \varepsilon^2, u/c, v/c, h_y/h_x \right\}. \tag{4.21}$$

For the first-order ($p = 1$) scheme, we can use the first-order restriction and prolongation operators. Then, $\psi(\hat{\mathbf{K}}) = 1/2$, for each of the operators $\hat{\mathbf{K}}^{HH}$, $\hat{\mathbf{K}}^{Hh}$, $\hat{\mathbf{K}}^{hH}$, $\hat{\mathbf{K}}^{(1)}$, and $\hat{\mathbf{K}}^{(2)}$. This number has been obtained by extensive numerical computations on the system of equations, and analytically by considering the fourth equation only. This is the same value as obtained for the two-grid operator of the method described in §2, using one smoothing step with damped Point-Jacobi (see also [11]).

To illustrate this result for the first-order scheme in the case of $\hat{\mathbf{K}}^{HH}$ and $\tilde{u} > 0$, $\tilde{v} > 0$, we use Taylor series to find

$$\hat{\mathbf{K}}_{1,1}^{HH} \simeq \frac{\frac{1}{2}(\tilde{u}\theta_x^2 + \tilde{v}\theta_y^2)}{\mathrm{i}(\tilde{u}\theta_x + \tilde{v}\theta_y)}. \tag{4.22a}$$

The numerator is the *truncation error* of the first-order scheme, the denominator the *exact operator*. If the latter is large enough, the right-hand side of (4.12) vanishes as θ_x and θ_y go to zero. On the other hand, if the exact operator becomes small, we can define $\alpha = \tilde{v}/\tilde{u} > 0$, let $\theta_x = \varepsilon\theta_1$ and $\theta_y = -\varepsilon\theta_1/\alpha + \varepsilon^{1+p}\theta_2$, and consider small ε and θ_2. The result is:

$$\hat{\mathbf{K}}_{1,1}^{HH} \simeq \tfrac{1}{2} + \mathrm{i}\tfrac{(1-\alpha)}{6\alpha}\theta_1\varepsilon - \mathrm{i}\tfrac{\alpha^2}{2(1+\alpha)}\theta_1^{-2}\theta_2. \tag{4.22b}$$

We conclude that the value $\psi(\hat{\mathbf{K}}) = 1/2$ occurs when the exact operator becomes of the order of the truncation error.

If the coarse-grid residual operators for $p = 2$ or $p = 3$ are first-order in the direction in which the coarsening has been carried out, and the restriction and prolongation operators are first-order, we find $\psi(\hat{\mathbf{K}}) = 1$ for each of the coarse-grid correction operators considered in this section.

For the third-order ($p = 3$) scheme, the coarse-grid residual operator and the restriction operator R for the residual are third-order, whereas the other restriction and prolongation operators ($\tilde{R}$, P, $\tilde{P}$) are first-order. In that case, $\psi(\hat{\mathbf{K}}) = 7/8 = 0.875$. Again, this value is based on analytical results for the fourth equation and numerical computations on the system.

The values of $\psi(\hat{\mathbf{K}})$ are lower limits for the worst-case multigrid convergence rates. Thus, the above shows that one can not design a multigrid scheme with a uniformly good convergence rate for a spatial discretisation based on second-order upwind differencing. For a third-order scheme, one might be able to obtain a convergence rate of at best $7/8$, which is not very impressive. However, these conclusions are too pessimistic, as the values of $\psi(\hat{\mathbf{K}})$ are dominated by those waves for which the exact operator becomes of the order of the truncation error. Because is does not make much sense to require convergence below the truncation error, the numbers found are not representative for the performance of the multigrid method.

The main problem is to find a way of measuring the convergence rate in comparison to the truncation error. I have not found a simple and elegant way to accomplish this in the framework of local mode analysis, but it can be easily done in the context of defect correction.

5. Defect correction

5.1. Convergence properties

The defect-correction technique can be used to solve the linear second-order problem $L_2\overline{u} = f_2$ by applying an iterative method for the first-order problem with operator L_1. If the iteration matrix for the first-order problem is M, then the iterations for the second-order problem are described by

$$v_{i+1} = [I - (I - M)L_1^{\dagger}L_2]v_i, \quad i \geq 0. \tag{5.1}$$

Here i is the iteration count, $v_i = \overline{u} - u_i$ the iteration error, and u_i the current guess of the solution.

There are several variants of the defect-correction technique (cf.[4]). In [7] and [8], a second-order upwind discretisation of Euler's equations is solved by a multigrid correction scheme designed for the linearisation of a first-order discretisation. The technique is used in combination with successive grid-refinement in [8], using second-order solutions during the refinement sequence. A variant that starts with a first-order solution and uses a nonlinear multigrid method as the first-order solver is described in [13] and [6]. The first-order solver is presented in [5]. This method has $O(N \log N)$ complexity, as the iteration error has to be reduced from $O(h)$, the accuracy of the initial first-order guess, to $O(h^2)$, the desired accuracy. Because the solver is not exact, not even for the long waves, this will require $O(\log N)$ iterations with the defect-correction technique. According to the authors, this does not seem to be significant in practice. It should be noted that the first-order solver of [5] can not handle alignment in subsonic flow, and that relaxation based on an exact linearisation of Osher's scheme, as advertised in [5], can lead to rather ill-conditioned matrices. A simple alternative is described in [11].

Defect correction does not provide good asymptotic convergence rates for the problem studied here. Even with an exact solver ($M = 0$), the expression $[I - L_1^{\dagger}L_2]$ can be close to I for certain waves. These waves are the same as those that caused bad convergence rates in the previous section. To illustrate this, consider the symbol of the fourth equation of (3.4). For $\tilde{u}\theta_x = -\tilde{v}\theta_y$, cf. (4.15b), and $\tilde{u} > 0$, $\tilde{v} > 0$, we obtain

$$1 - \hat{L}_2/\hat{L}_1 \simeq 1 - \mathrm{i}\tfrac{1}{2}(\kappa - \tfrac{1}{3})(\theta_x + \theta_y). \tag{5.2}$$

This shows that the defect-correction technique can not provide a uniformly good convergence rate for Euler's equations. The problem here is the same as in the previous section: if the operator

becomes of the order of the truncation error, the convergence rate deteriorates. But at that point, convergence is no longer important because the iteration error has become of the order of the discretisation error, which is accurate enough.

The framework of the defect-correction technique allows us to obtain estimates about convergence to the level of the truncation error, in contrast to the approach of the previous section. To show this, we first introduce some notation. Let the linear problem be $Lu = f$. The discrete representation of the solution on a grid corresponding to level l is $\tilde{I}_p^l u$, with an order of accuracy p. The discrete operator is L_p^l, and $f_p^l = I_p^l f$. We assume that we have some iterative scheme M^l for solving the problem with accuracy $p = p_1$. Let

$$\check{M}^l \equiv L_{p_1}^l M^l (L_{p_1}^l)^\dagger, \quad \|\check{M}^l\| \leq \overline{\lambda}_r, \tag{5.3}$$

where the convergence rate $\overline{\lambda}_r$ should be well below 1. The similarity transform based on $L_{p_1}^l$ is introduced to allow for singular problems. Components of the solution that lie in the null-space of $L_{p_1}^l$, denoted by $\mathcal{N}(L_{p_1}^l)$ are hereby ignored. Note that a necessary condition for boundedness of $(L_{p_1}^l)^\dagger L_{p_2}^l$ is: $\mathcal{N}(L_{p_1}^l) \subset \mathcal{N}(L_{p_2}^l)$.

The numerical solution $\overline{u}^l$ of the problem with order of accuracy $p_2 > p_1$ obeys $L_{p_2}^l \overline{u}^l = f_{p_2}^l = I_{p_2}^l f$. We have not used the subscript p_2 here for u^l. Its discretisation error is $e_p^l = \tilde{I}_p^l u - \overline{u}^l$, and the corresponding truncation error of the residual is defined by $\tau_p^l = L_p^l e_p^l = (L_p^l \tilde{I}_p^l - I_p^l L)u$. The current guess of the solution is u_i^l, where i is the iteration count. The iteration error $v_i^l = \overline{u}^l - u_i^l$, and the total error is $z_i^l = \tilde{I}_{p_2}^l u - u_i^l$. The current residual $r_i^l = f_{p_2}^l - L_{p_2}^l u_i^l = L_{p_2}^l v_i^l$. The equivalent of Eq.(5.1) for the residual is

$$r_{i+1}^l = L_{p_2}^l [I - (I - M^l)(L_{p_1}^l)^\dagger L_{p_2}^l](L_{p_2}^l)^\dagger r_i^l, \quad i \geq 0. \tag{5.4a}$$

Using $r^l = L_{p_2}^l z^l - \tau_{p_2}^l$, this can be rewritten as

$$L_{p_2}^l z_{i+1}^l = L_{p_2}^l (L_{p_1}^l)^\dagger \left[\check{M}^l L_{p_2}^l z_i^l + (I - \check{M}^l)\tau_{p_2}^l\right] + L_{p_2}^l \left[I - (L_{p_1}^l)^\dagger L_{p_2}^l\right] z_i^l. \tag{5.4b}$$

The first term on the right-hand side in square brackets clearly allows for convergence down to the truncation error. The last term may cause problems, though. If $L_{p_1}^l$ is nonsingular or if the null-space of $L_{p_1}^l$ is a subset of the null-space of $L_{p_2}^l$, the last term can be rearranged as

$$(I - L_{p_2}^l (L_{p_1}^l)^\dagger) L_{p_2}^l z_i^l = L_{p_2}^l (L_{p_1}^l)^\dagger (L_{p_1}^l - L_{p_2}^l) z_i^l \tag{5.4c}$$

In a Full Multigrid code, it may be assumed that the initial guess of the solution has an error of the order of the discretisation error. Therefore, we let $\|L_{p_2}^l z_i^l\| = \alpha_i^l \|\tau_{p_2}^l\|$, where α_i^l is assumed to be $O(1)$. Also, we assume that $\|L_{p_2}^l (L_{p_1}^l)^\dagger\| \leq C_{2,1}$, where $C_{2,1}$ is $O(1)$. It follows from (5.4c) that

$$\alpha_{i+1}^l \|\tau_{p_2}^l\| \leq \overline{\lambda}_r C_{2,1} \alpha_i^l \|\tau_{p_2}^l\| + (1 + \overline{\lambda}_r) C_{2,1} \|\tau_{p_2}^l\| + C_{2,1} \|(L_{p_1}^l - L_{p_2}^l) z_i^l\|. \tag{5.5}$$

The first term on the right-hand side decreases after each iteration if $\overline{\lambda}_r C_{2,1} < 1$. The second term is of the order of the truncation error. The last term can be neglected if

$$\|(L_{p_1}^l - L_{p_2}^l) z_i^l\| \leq \alpha_i \|L_{p_1}^l - L_{p_2}^l\| \, \|\tau_{p_2}^l\| = O(h^{p_1 + p_2}). \tag{5.6}$$

Assuming that $\|\tau_{p_2}^l\| = O(h^{p_2}) \neq 0$, which excludes certain trivial solutions, and neglecting the term in (5.6), we get

$$\alpha_i^l \leq (\overline{\lambda}_r C_{2,1})^i \alpha_0^l + (1 + \overline{\lambda}_r) C_{2,1} \beta(\overline{\lambda}_r C_{2,1}, i), \quad \beta(x, i) = \frac{1 - x^i}{1 - x}. \tag{5.7}$$

κ	$C_{2,1}$	$\phi(\frac{1}{2},*,C_{2,1},\infty,\infty)$	$i(<10\%)$
1	1.00	(3.00)	(6)
$\frac{1}{3}$	1.06	3.39	6, 7
0	1.15	4.10	7
-1	2.00	–	–

Table 1. *The constant $C_{2,1}$, for various values of κ, determines the best accuracy one can obtain with the defect correction technique. The accuracy is measured by $\phi(\overline{\lambda}_r, p_2, C_{2,1}, i, l)$ times the norm of the truncation error. The third column gives the asymptotic values, which are independent of p_2, the order of accuracy of the discretisation. The last row gives the number of cycles needed to obtain this accuracy within 10%. The convergence estimate for $\kappa = 1$ can not be justified and is only included for reference. The two values for $\kappa = 1/3$ refer to $p_2 = 2$ and 3, respectively. Other values of κ result in second-order accuracy ($p_2 = 2$).*

Therefore, the defect-correction technique can provide a solution with a total error which is at best a factor $(1 + \overline{\lambda}_r)C_{2,1}\beta(\overline{\lambda}_r C_{2,1}, i)$ times the truncation error.

Next consider the Full Multigrid method. We like to obtain an estimate of α_i^l for a fixed iteration count. Given a solution u_i^{l-1}, we obtain an initial guess on level l through interpolation: $u_0^l = I_{l-1}^l u_i^{l-1}$. Here we assume that the order of interpolation is at least $(p_2 + 1)$. If $\|\tau_{p_2}^l\| = 2^{p_2}\|\tau_{p_2}^{l-1}\|$, we find that

$$\alpha_i^l \le \zeta^l \alpha_i^0 + \phi(\overline{\lambda}_r, p_2, C_{2,1}, i, l), \tag{5.8a}$$

where

$$\zeta = 2^{p_2}(\overline{\lambda}_r C_{2,1})^i, \quad \phi(\overline{\lambda}_r, p_2, C_{2,1}, i, l) = (1 + \overline{\lambda}_r)C_{2,1}\beta(\overline{\lambda}_r C_{2,1}, i)\beta(\zeta, l). \tag{5.8b}$$

Here we have ignored terms of $O(h)$ or smaller.

Note that the above does not represent a convergence proof. It merely describes convergence of the residual to the level of the truncation error. The description is based on §5.2, §14.2, and §14.3 in [4].

5.2. Example

To obtain quantatative estimates, we consider a second-order discretisation ($p_2 = 2$) and a first-order solver ($p_1 = 1$) with a multigrid convergence rate $\overline{\lambda}_r = \frac{1}{2}$. Note that the multigrid convergence rate is usually larger than the two-level convergence rate. The number 0.5 obtained for the method in §2 corresponds to the two-level rate. However, the numerical experiments in [11] show a multigrid convergence rate well below 0.5, and this motivates the present choice for $\overline{\lambda}_r$.

According to the Appendix, we have $\mathcal{N}(L_1) = \mathcal{N}(L_2)$ for $\kappa < 1$. If $\kappa = 1$, the null-space of L_2 contains $\mathcal{N}(L_1)$, but is larger. Eq.(5.4c) still holds, but the estimate (5.6) may break down because of the checker-board mode. This mode may result in an initial guess after grid-refinement which is not smooth enough. Therefore, the use of a scheme with $\kappa = 1$ (central differencing) is not recommended. We will nevertheless include it in our estimates.

Results are listed in Table 1. The values of $C_{2,1}$ are obtained numerically by using the norm (4.9) on $\hat{L}_1^\dagger \hat{L}_2$. For the fourth equation of the system (3.4), we obtain $C_{2,1} = 1$ for $\kappa = 1$, $C_{2,1} = \sqrt{9/8}$ for $\kappa = 1/3$, $C_{2,1} = \sqrt{4/3}$ for $\kappa = 0$, and $C_{2,1} = 2$ for $\kappa = -1$, which happen to

agree with the numerical results. The best result one can obtain for convergence of the residual in terms of the truncation error is asymptotically determined by $\phi(\frac{1}{2}, *, C_{2,1}, \infty, \infty)$, if one assumes that the solution on the coarsest level ($l = 0$) is determined exactly, i.e., $\alpha_\infty^0 = 0$. The asterisk indicates that this asymptotic value is independent of p_2. It should be noted that the result for $\kappa = 1$ can not be justified, as already mentioned. For $\kappa = -1$, the product $\overline{\lambda}_r C_{2,1}$ becomes 1 and convergence is lost. The last column of Table 1 list the number of iterations required reach the asymptotic result within 10%. This, or a slightly larger value, can be used as the number of cycles to be carried out in practical computations. The result $i(< 10\%) = 6$ for $\kappa = 1/3$ is obtained with $p_2 = 2$. For $p_2 = 3$, we obtain $i(< 10\%)$=7.

If the solution is not sufficiently smooth, the assumption (5.4c) will be violated because of the high frequencies. This, however, can be easily repaired by some additional smoothing. One or more smoothing steps can be applied to the higher-order residual between defect-correction steps. A simple smoother is Point-Jacobi, but this scheme has a long wave instability for the higher-order upwind discretisation. Stability can be obtained by a Two-Stage method:

$$\begin{aligned} u_* &= u_i - \beta_1 N^{-1} r_i, \\ u_{i+1} &= u_i - \beta_2 N^{-1} r_*. \end{aligned} \tag{5.9}$$

Here $N = |A| + |B|$. The relaxation parameters β_1 and β_2 can be chosen in such a way that the Two-Stage scheme is stable and that the smoothing rate

$$\overline{\mu} = \max\{\rho(\hat{S}^{MS}) : \tfrac{1}{2}\pi \le |\theta_x| \le \pi, \tfrac{1}{2}\pi \le |\theta_y| \le \pi, u/c, v/c, h_y/h_x\}, \tag{5.10}$$

is as small as possible. Here

$$\hat{S}^{MS} = I - \beta_2 N^{-1} \hat{L}_{p_2} (I - \beta_1 N^{-1} \hat{L}_{p_2}), \tag{5.11}$$

is the symbol of the relaxation operator. Note that N^{-1} should be read as $N^\dagger$, as N becomes singular for $u = v = 0$. An optimal choice for $\kappa = 0$ is $\beta_1 = 2/5 = 0.400$, $\beta_2 = 10/13 = 0.769$, resulting in a smoothing rate $\overline{\mu} = 9/13 = 0.692$. For $\kappa = 1/3$, a nearly optimal choice is $\beta_1 = 3/5 = 0.600$, $\beta_2 = 10/11 = 0.909$, which lets $\overline{\mu} = 25/33 = 0.758$.

It should be noted that these values are not necessarily optimal in the presence of a limiter. The use of limiters makes the scheme nonlinear, even if applied to linear equations with constant coefficients. A Point-Jacobi scheme applied to the high-resolution scheme can be TVD stable if limiters are used, in contrast to the result of linear local mode analysis (cf.[3]). On the other hand, nonlinearities as sonic lines and shocks may require values of β_1 and β_2 smaller than those mentioned above to provide stability for the Two-Stage scheme.

6. Discussion

Some problems in the application of the multigrid method to Euler's equations of gas dynamics have been identified by local mode analysis for the linear constant-coefficient case. Alignment can be overcome by line relaxation. A nonlinear alternative based on semi-coarsening requires $O(N)$ operations per multigrid correction cycle. In this way, acceptable convergence rates can be obtained for a first-order upwind discretisation.

For higher-order schemes, it appears difficult, if not impossible, to obtain good asymptotic convergence rates. This is mainly due to waves perpendicular to stream-lines. For these waves, the exact operator vanishes and convergence is dominated by the truncation error. Convergence to machine-zero will be very slow or impossible. However, convergence to the level of the truncation error can be easily obtained by defect correction.

If one insists on convergence to machine-zero, the spatial discretisation of Euler's equations must be improved such that the null-spaces for the discrete and exact operator coincide. Central differencing provides this at 45°, but also introduces the checker-board mode, which is too much. The use of rotated differences may be an improvement, but it seems impossible to match the null-spaces for angles other than some integer multiple of 45°. Therefore, convergence to machine-zero be better abandoned. Note that this statement refers to the worst case. In practical computations, convergence to machine-zero can be, and has been, obtained.

The implementation of the method outlined on §5 for the nonlinear case is discussed in [12]. Apart from technical difficulties, there do not appear to be any fundamental obstacles for multigrid convergence, as long as one is willing to give up convergence to machine-zero.

Appendix. The singularities of $\hat{L}^{h_x,h_y}$

Lemma. *The linearised residual operator $\hat{L}^{h_x,h_y}$, with $0 \le s_x \le 1$, $0 \le s_y \le 1$, and $\kappa < 1$, is singular only in each of the following cases:*

$$\begin{aligned}
&(i) && \hat{T}_x = 1, \hat{T}_y = 1 \\
&(ii) && \hat{T}_x \neq 1, \hat{T}_y = 1: \ u = -c \text{ or } u = 0 \text{ or } u = c; \\
&(iii) && \hat{T}_x = 1, \hat{T}_y \neq 1: \ v = -c \text{ or } v = 0 \text{ or } v = c; \\
&(iv) && \hat{T}_x \neq 1, \hat{T}_y \neq 1: \ u = v = 0.
\end{aligned}$$

The corresponding null-spaces do not depend on s_x, s_y, and κ.

Proof. In the first case, the linearised residual operator $\hat{L}^{h_x,h_y} = 0$. Its null-space is clearly independent of s_x, s_y, and κ. In the second case we have $\hat{L}^{h_x,h_y} = \hat{L}_x^{h_x}$. This expression can be diagonalised by Q_1, yielding eigenvalues

$$\frac{1}{h_x}\lambda_{1,l} D(\hat{T}_x, s_x, \kappa), \quad l = 1, \ldots, 4. \tag{A.1}$$

Because $D(\hat{T}_x, s_x, \kappa) \neq 0$ for $\hat{T}_x \neq 1$, this expression only vanishes if $\lambda_{1,l} = 0$, i.e., if one of the eigenvalues of A vanishes. The third case is proven in the same way.

For case *(iv)* we consider the real part of the operator $\hat{L}^{h_x,h_y}$. Using the fact that $\mathrm{Re}\,\hat{D}(\hat{T}, s, \kappa) = \mathrm{Re}\,\hat{D}(\hat{T}^{-1}, s, \kappa)$, we find that

$$\mathrm{Re}\,\hat{L}^{h_x,h_y} = \mu_1|A| + \mu_2|B|, \quad \mu_1 = \frac{1}{h_x}\mathrm{Re}\,\hat{D}(\hat{T}_x, s_x, \kappa), \quad \mu_2 = \frac{1}{h_y}\mathrm{Re}\,\hat{D}(\hat{T}_y, s_y, \kappa). \tag{A.2}$$

From (3.12) it can be seen that $\mathrm{Re}\,\hat{D}(\hat{T}, s, \kappa)$ vanishes only if $\hat{T} = 1$ and is positive otherwise. Thus, both μ_1 and μ_2 are positive. The expression $\mu_1|A| + \mu_2|B|$ has a zero eigenvalue only if $u = v = 0$. In that case, the fourth equation vanishes. The corresponding null-space is clearly independent of s_x, s_y, and κ.

For the remaining 3×3 system, that is obtained by dropping the fourth row and fourth column of $\hat{L}^{h_x,h_y}$, we obtain a non-zero determinant, implying that this part of the system is not singular. To show that the determinant is non-zero, we consider, in addition to (A.2), the imaginary part of $\hat{L}^{h_x,h_y}$. Using the fact that $\mathrm{Im}\,\hat{D}(\hat{T}, s, \kappa) = -\mathrm{Im}\,\hat{D}(\hat{T}^{-1}, s, \kappa)$, we obtain

$$\mathrm{Im}\,\hat{L}^{h_x,h_y} = \nu_1 A + \nu_2 B, \quad \nu_1 = \frac{1}{h_x}\mathrm{Im}\,\hat{D}(\hat{T}_x, s_x, \kappa), \quad \nu_2 = \frac{1}{h_y}\mathrm{Im}\,\hat{D}(\hat{T}_y, s_y, \kappa). \tag{A.3}$$

For $u = v = 0$, the 3×3 system becomes

$$\begin{pmatrix} \mu_1 c & 0 & \mathrm{i}\nu_1 c \\ 0 & \mu_2 c & \mathrm{i}\nu_2 c \\ \mathrm{i}\nu_1 c & \mathrm{i}\nu_2 c & (\mu_1 + \mu_2) \end{pmatrix}, \tag{A.4a}$$

which has a determinant

$$c^3 \left(\mu_1(\mu_2^2 + \nu_2^2) + \mu_2(\mu_1^2 + \nu_1^2) \right), \tag{A.4b}$$

which is positive, because μ_1 and μ_2 are positive. Thus, the 3×3 system is non-singular. □

References

[1] W. K. Anderson, J. L. Thomas, B. van Leer, *A comparison of finite volume flux vector splittings for the Euler equations*, AIAA Paper No. 85-0122, presented at the AIAA 23rd Aerospace Sciences Meeting, January 1985, Reno, Nevada.

[2] A. Brandt, *Guide to Multigrid Development*, Lecture Notes in Mathematics 960 (1981), 220-312.

[3] S. R. Chakravarthy and S. Osher, *Computing with High-Resolution Upwind Schemes for Hyperbolic Equations*, in *Large-Scale Computations in Fluid Mechanics*, Lectures in Applied Mathematics 22, eds. B. E. Engquist, S. Osher, R. C. J. Somerville, American Math. Society, Providence, Rhode Island, 1985, pp. 57-86 (part 1).

[4] W. Hackbusch, *Multi-Grid Methods and Applications*, Springer Series in Computational Mathematics 4 (1985), Springer Verlag, Berlin/Heidelberg.

[5] P. W. Hemker and S. P. Spekreijse, *Multiple grid and Osher's scheme for the efficient solution of the steady Euler equations*, Appl. Num. Math. 2 (1986), 475-493.

[6] B. Koren, *Defect Correction and Multigrid for an Efficient and Accurate Computation of Airfoil Flows*, J. Comp. Phys. 77 (1988), 183-206.

[7] W. A. Mulder, *Multigrid Relaxation for the Euler Equations*, J. Comp. Phys. 60 (1985), 235-252.

[8] W. A. Mulder, *Computation of the Quasi-Steady Gas Flow in a Spiral Galaxy by Means of a Multigrid Method*, Astron. Astrophys. 156 (1986), 354-380.

[9] W. A. Mulder, *Analysis of a multigrid method for the Euler equations of gas dynamics in two dimensions*, in *Multigrid Methods: Theory, Applications, and Supercomputing*, ed. S. McCormick, Marcel Dekker, New York (1988).

[10] W. A. Mulder, *A note on the use of Symmetric Line Gauss-Seidel for the upwind differenced Euler equations*, submitted to SIAM J. Sci. Stat. Comput.

[11] W. A. Mulder, *A new multigrid approach to convection problems*, CAM Report 88-04 (1988), UCLA. J. Comp. Phys., in press.

[12] W. A. Mulder, *A high resolution Euler solver*, in prep.

[13] S. P. Spekreijse, *Multigrid Solution of the Steady Euler Equations*, Ph. D. Thesis, Centrum voor Wiskunde en Informatica, Amsterdam (1987).

[14] B. van Leer, *Upwind-difference methods for aerodynamic problems governed by the Euler equations*, in *Large-Scale Computations in Fluid Mechanics*, Lectures in Applied Mathematics 22, eds. B. E. Engquist, S. Osher, R. C. J. Somerville, American Math. Society, Providence, Rhode Island, 1985, pp. 327-336 (part 2).